

**EUROPEAN ORGANISATION FOR THE
SAFETY OF AIR NAVIGATION**



DFS Deutsche Flugsicherung GmbH



**Preliminary study of the Impact
of the Emissions of Space
Stations in the Radio
Navigation-Satellite Service into
the Radars operating in the
Band 1215 – 1300 MHz**

Edition	:	1.7
Edition Date	:	08/04/2002
Status	:	Released Issue
Class	:	General Public

DOCUMENT IDENTIFICATION SHEET

DOCUMENT DESCRIPTION

Document Title

Study of the impact of the Emissions of Space Stations in the Radio Navigation-Satellite Service into the Radars operating in the Band 1215 – 1300 MHz

DELIVERABLE REFERENCE NUMBER: COM/SP/STUDY/DFS/020212

**PROGRAMME
REFERENCE INDEX:**

EDITION: 1.7

**EDITION
DATE:** 08/04/2002

Abstract

Preliminary theoretical evaluation of the maximal RNSS Power Flux Density (PFD) to protect L-band Radar has been presented to ITU, CEPT and ICAO. The theoretical PFD value was derived from the radar interference protection limit as stipulated by ITU-R Recommendation M.1461 for the worst case scenario where the satellite transceiver is in the same azimuth than the aircraft target and when the central frequency of the satellite transceiver and of the radar receiver is the same. The purpose of this study is to provide more experimental material to confirm the theoretical calculations derived from the ITU-R Recommendation M.1461. The impact of the simulated RNSS interference signals was investigated primarily by measuring the loss of the probability of detection (P_D) of targets, compared with the second undisturbed channel of a Air Traffic Control Radar. The measurements confirm the I/N ratio limit as per ITU-R Recommendation M.1463 derived by applying the methodology given in the ITU-R recommendation M.1461 to protect radar from wide-band noise like signals for the worst case scenario. For the RNSS narrow-band signals which are not accounted for in the above mentioned ITU-R Recommendations, the measurements indicate an I/N ratio more stringent than for the wide-band signals. The Pfd value derived from the measurement on the worst case scenario shall be considered indicative. Further work is needed to determine the probability of occurrence of the worst case scenario where the satellite transceiver is in the same azimuth than the aircraft target and to determine the impact on the complete radar chain in order to document and quantify the potential risk on ATC operations.

Keywords

L-band Radar, Power Flux Density Limit, Interference Susceptibility Measurements, Satellite Navigation Systems, GPS, GLONASS, GALILEO, DFS

DOCUMENT STATUS AND TYPE

STATUS	CLASSIFICATION
Working Draft <input type="checkbox"/>	General Public <input checked="" type="checkbox"/>
Draft <input type="checkbox"/>	EATMP <input type="checkbox"/>
Proposed Issue <input type="checkbox"/>	Restricted <input type="checkbox"/>
Released Issue <input checked="" type="checkbox"/>	

PROJECT COORDINATION		
Organisation	Interest	Contact Name
DFS Deutsche Flugsicherung GmbH	Author	Dr.-Ing. Felix Butsch
	Contributors	Ulrich Bonerz, Helmut Günzel, Wilhelm Gurt, Hans Nessler
	Quality Review	Torsten Jacob
EUROCONTROL	Client contract Management	C.Pelmoine
	Quality Review	A.Stratton
	Technical Expert	S.Adamopoulos

DOCUMENT APPROVAL

The following table identifies all management authorities who have successively approved the present issue of this document.

DFS Deutsche Flugsicherung

AUTHORITY	NAME AND SIGNATURE	DATE
S. Naerlich		
J. Dzuba		
F. Butsch		

EUROCONTROL

AUTHORITY	NAME AND SIGNATURE	DATE
Head of DIS/COM Unit	G.BAILEY	
Head of DIS/SUR Unit	M.REES	
Spectrum Manager	C.PELMOINE	
Radar Expert	S.ADAMOPOULOS	
Quality review	A.STRATTON	

DOCUMENT CHANGE RECORD

The following table records the complete history of the successive editions of the present document.

EDITION	DATE	REASON FOR CHANGE	SECTIONS PAGES AFFECTED
1.0	02/10/01	First proposed issue	All
1.1	11/10/01	Amendments and modifications dealing with the dependence of the I/N ratio of the bandwidth	All
1.2	10/01/02	Modifications and refinements for presentation at CEPT SE28	All
1.3	12/02/02	Modifications following quality review.	All [Exec. Summary, Section 2 and 5.]
1.4	08/03/02	Removal of results based on data recorded over 5 minutes	Section 4.3, Appendix D
1.5	18/03/02	Modifications, made by Butsch as discussed by phone on with Pelmoine, Adamopoulos, Stratton 18/03/02	[Section 4.3 and appendix B
1.6	19/03/02	Minor editorial changes and reformatting	Exec.Summary, Section 5, Annex B
1.7	08/04/02	Modifications following quality review, to accommodate comments from EC Galileo STF	Exec.Summary, Section 5

Copyright notice

© 2002 European Organisation for the Safety of Air Navigation (EUROCONTROL). All rights reserved.
No part of this publication may be reproduced, stored in a retrieval system, or transmitted in any form or by any means, electronic, mechanical, photocopying, recording or otherwise, without the prior written permission of EUROCONTROL.

TABLE OF CONTENTS

DOCUMENT IDENTIFICATION SHEET	ii
DOCUMENT APPROVAL	iii
DOCUMENT CHANGE RECORD.....	iv
EXECUTIVE SUMMARY	4
1. INTRODUCTION.....	6
2. REQUIREMENTS.....	6
3. APPROACH	7
3.1 Description of the measurement method	7
3.2 Description of the Satellite navigation signals used for the measurements.....	9
4. RESULTS / FINDINGS	11
4.1 Considerations about the Radar antenna	11
4.2 Interference impact on the Radar receiver.....	11
4.2.1 Considerations about the impact of various types of interference signals.....	11
4.2.2 Considerations about potential saturation of the low noise amplifier	13
4.2.3 Measured impact at the IF stage output	13
4.3 Interference impact on Radar processing	165
4.4 Interference conditions in Germany	20
5. CONCLUSION / RECOMMENDATIONS	22
6. REFERENCES	23
APPENDIX A – DESCRIPTION OF RADAR AND MEASUREMENT SET-UP.....	24
APPENDIX B – THEORETICAL BACKGROUND	32
APPENDIX C – ABBREVIATIONS	36
APPENDIX D – SELECTED MEASUREMENT RESULTS.....	38

EXECUTIVE SUMMARY

PURPOSE

The ITU World Radiocommunication Conference 2000 (WRC-2000) invited with its Resolution 606 the Radiocommunication Sector to conduct, as a matter of urgency and in time for WRC-03, the appropriate technical, operational and regulatory studies, including an assessment for a power flux-density limit concerning the operation of radionavigation-satellite service (space-to-Earth) systems in the frequency band 1215 – 1300 MHz in order to ensure that the radionavigation-satellite service (space-to-Earth) will not cause harmful interference to the radionavigation and the radiolocation services.

Preliminary theoretical evaluation of the maximal RNSS Power Flux Density (PFD) to protect L-band Radar has been presented to ITU, CEPT and ICAO. In spite of one existing RNSS system having transmitted at its current power level for over 12 years and having not caused interference to other users of the band, the presentations noted the discrepancy (30 to 40 dB) between the theoretical PFD value and the PFD produced by existing GPS and GLONASS satellites. The theoretical PFD value was derived from the radar interference protection limit as stipulated by ITU-R Recommendation M.1461 for the worst case scenario where the satellite transceiver is in the same azimuth than the aircraft target and when the central frequency of the satellite transceiver and of the radar receiver is the same.

The purpose of this study is to provide more experimental material to confirm the theoretical calculations derived from the ITU-R Recommendation M.1461.

METHOD

For this purpose, measurements have been conducted to determine the sensitivity to RNSS signals of ATC Radar operated by the German Air Navigation Services DFS at a carrier frequency of 1259 MHz. The simulated RNSS signals were centred at 1259 MHz and injected at the input of the low noise amplifier of the radar receiver, with the antenna rotating and at specific times corresponding to 12 selected azimuth directions with the highest observed air-traffic density.

The impact of the simulated RNSS interference signals was investigated primarily by determination of the loss of the probability of detection (P_D) of targets, -compared with the second undisturbed channel of the radar at 1343 MHz. The probability of detection was assessed using the EUROCONTROL SASS-C software tool which reconstructs individual aircraft trajectories by chaining and smoothing individual plots, extracted after each radar scan. Comparison of the position and presence of those plots with their associated trajectory allows counting the number of hits and misses from which P_D is derived.

CONCLUSIONS / RECOMMENDATIONS

German civil ATC Radars utilise carrier frequencies in the band 1250 to 1260 MHz. Within this band, at the time of the study (August – September 2001), the only satellite navigation signal that could be received, was transmitted by a GLONASS satellite with the channel number 10. Despite the fact, that the measurements with simulated RNSS signals have shown a loss of probability of detection up to 25 % in the direction of the satellite transmitter, an impact was not reported in the past. The reasons for this might be, that people responsible for this radar system were not aware of the problem, that only one RNSS satellite was transmitting near the radar carrier frequency, and that only a narrow angle segment with a width of 1° to 2°, is potentially affected.

The measurements confirm the I/N ratio limit as per ITU-R Recommendation M.1463 derived by applying the methodology given in the ITU-R recommendation M.1461 to protect radar from wide-band noise like signals for the worst case scenario. For the RNSS narrow-band signals which are not accounted for in the above mentioned ITU-R Recommendations, the measurements indicate an I/N ratio more stringent than for the wide-band signals.

The Pfd value derived from the measurement on the worst case scenario shall be considered indicative. Further work is needed to determine the probability of occurrence of the worst case scenario where the satellite transceiver is in the same azimuth than the aircraft target and to determine the impact on the complete radar chain in order to document and quantify the potential risk on ATC operations.

1. INTRODUCTION

In ITU, CEPT and ICAO, theoretical evaluation of maximal RNSS Power Flux Density (PFD) to protect L-band Radar were presented. All presentations noted the huge discrepancy (30 to 40 dB) between the PFD produced by existing GPS and GLONASS satellites on the Earth's surface and theoretical PFD values derived from radar interference protection limit as stipulated by ITU-R Recommendation M.1461. Therefore there was a need to investigate this issue by practical measurements.

Specifically the aim and main tasks of this study were:

To determine the RNSS PFD necessary to protect the L-band Radar by following means:

- Measurement of RNSS (GLONASS L1-C/A, GPS L2-C/A, GPS L2-P and Galileo E6) simulated signal impact on a typical L-band ATC Radar located in Germany
- To consider the output at the front-end receiver to determine interference impact on front-end receiver and to determine I/N ratio at this stage.
- To consider the output after the Radar processing to evaluate the interference impact on Radar processing (Probability of detection, P_D and probability of false alarm, P_{FA}).
- To compare the result with expected real RNSS PFD and with the calculated PFD limit and to evaluate PFD limit to be proposed in ICAO and CEPT/ITU.

2. REQUIREMENTS

The work comprises the following work packages (WPs):

WP 1 Preparation of measurement:

- To prepare the measurements, laboratory tests are conducted to find the optimal way to simulate the satellite navigation signals.
- For the calculation of the Power Flux Density PFD from a measured interference power, the insertion loss between the antenna and the interface, where the interference signal will be fed needs to be determined. For this purpose, the loss of the wave guide and other components in front of the low noise amplifier is to be determined. The results are validated by measurement of the received power of a test signal transmitted via air.

WP 2 Conduction of measurements:

Measurement of the impact of simulated satellite navigation signals on a typical primary Radar receiver by injection of the simulated interference signals in the signal path of the Radar:

- Determination of the interference impact on the receiver.
- Gathering of data like spectra of the signals, increase of the noise floor and recording of data provided by the sensor data processor etc. Simultaneously recording of data from undisturbed channels, like second primary Radar channel and secondary Radar.

WP 3 Measurement Analysis and Conclusion:

The measured and recorded data in WP2 are processed and evaluated in order:

- to determine the interference impact on Radar processing (PD, PFA) by comparing the detection performance before and after the injection of the interference signal
- to determine the maximal PFD limit to protect L-band Radar using SASS-C 5.2
- to compare the result with expected real RNSS PFD using SASS-C 5.2
- to make recommendation for EUROCONTROL, ICAO, ITU and CEPT

3. APPROACH

3.1 Description of the measurement method

For the measurements, a DFS owned primary Radar station of the type SREM (Surveillance Radar Equipment, details see Appendix A) has been used. For operational reasons the Radar station Grosshaager Forst near Munich (Germany) has been selected to carry out the measurements. This is one out of six Radar stations of type SRE-M currently used by DFS. The selected Radar station has two primary Radar channels, one with a centre frequency of 1259 MHz (in the band under consideration of 1215 to 1300 MHz) and one at 1343 MHz (outside this band). In addition a Secondary Surveillance Radar (SSR) is co-located. Simulated interference signals were only fed in the 1259 MHz channel, whereas the 1343 MHz channel serves as a reference. The simulated interference signals were fed-in in front of the Low Noise amplifier (LNA) by means of a directional coupler at specific times corresponding to 12 selected azimuth directions with the highest observed air-traffic density (see Appendix A).

The impact of the simulated RNSS interference signals was investigated primarily by determination of the loss of the probability of detection (P_D) of targets, compared with the second undisturbed channel of the Radar at 1343 MHz. The probability of detection was assessed using the EUROCONTROL SASS-C software tool which reconstructs individual aircraft trajectories by chaining and smoothing individual plots, extracted after each radar scan. Comparison of the position and presence of those plots with their associated trajectory allows counting the number of hits and misses from which P_D is derived.

From the signal power of these signals the values of the associated Power Flux Density (PFD) at the antenna and the Interference to Noise power ratio (I/N) within the intermediate frequency bandwidth were determined (calculations see Appendix B). Great care was taken to determine the insertion loss between the input of the LNA and the antenna accurately. Furthermore the transfer function between the input of the LNA input and the output of the intermediate frequency stage was measured (Appendix A).

3.2 Description of the Satellite navigation signals used for the measurements

Simulated satellite navigation signals of different bandwidths, according to the various cases (GPS-L2, GLONASS-L2, as well as Galileo E6, see Fig. 1 and Tab. 1) were used to artificially interfere with the target echoes received by a Radar station).

The Radar channel used for the investigations (1259 MHz) is not centred with any of the currently existing or planned satellite signals under consideration. At least theoretically, a randomly picked Radar anywhere in the world in the frequency range 1215 to 1300 MHz could operate on the same centre frequency as any of the satellite signals discussed here. For this reason and to assess the worst case the simulated satellite navigation signals were centred with the centre frequency to the Radar channel at 1259 MHz (see Tab. 1, sources: for GPS properties see ITU-R M.1088 [Ref. 7], for GLONASS ITU R M.1317 [Ref. 8]).

According to the result of the WRC2000 [Ref.10], GALILEO E6 will make use of the band 1260 to 1300 MHz. The actual signal properties were in August 2001 as the measurements were carried out still under discussion. Binary phase shift keying (BPSK) and Binary Offset Carrier Modulation (BOC) as well as various code clock frequencies had been proposed. For the interference susceptibility measurements, a BPSK modulated signal with a code clock frequency of 20.46 MHz centred around 1259 MHz was chosen. Such a signal could be easily generated by the available signal generator and makes use of an approx. 40 MHz broad frequency range, which fits well in the band allocated for Galileo E6 at WRC2000 (Fig. 1).

Tab. 1: Properties of simulated signals

Signal	Properties of the real signals / Status of the signal	Properties of the simulated signals (centred around the Radar frequency of 1259 MHz)
GPS-L2 C/A-Code	$f_{HF} = 1227.6$ MHz, $f_C = 1.023$ MHz	$f_{HF} = 1259$ MHz $f_C = 1.023$ MHz
	To be implemented on GPS IIR-M satellites as well as on future satellite types like IIF and III. First satellite with this option to be launched in 2003, full constellation in 2008	
GPS-L2 P-Code	$f_{HF} = 1227.6$ MHz, $f_C = 10.23$ MHz	$f_{HF} = 1259$ MHz $f_C = 10.23$ MHz
	Currently active	
GLONASS- L2 C/A-Code	$f_{HF} = 1246 + k \cdot 0.4375$ MHz, where the k is the channel number k = -7 to 12 (after 2005: -7 to +4) $f_C = 0.511$ MHz	$f_{HF} = 1259$ MHz $f_C = 0.511$ MHz
	Currently active	
GALILEO-E6	$f_{HF} = 1278.75$ MHz $f_C = 20.46$ MHz	$f_{HF} = 1259$ MHz $f_C = 20.46$ MHz
	One among other options to be implemented in the future. Operational in 2008	

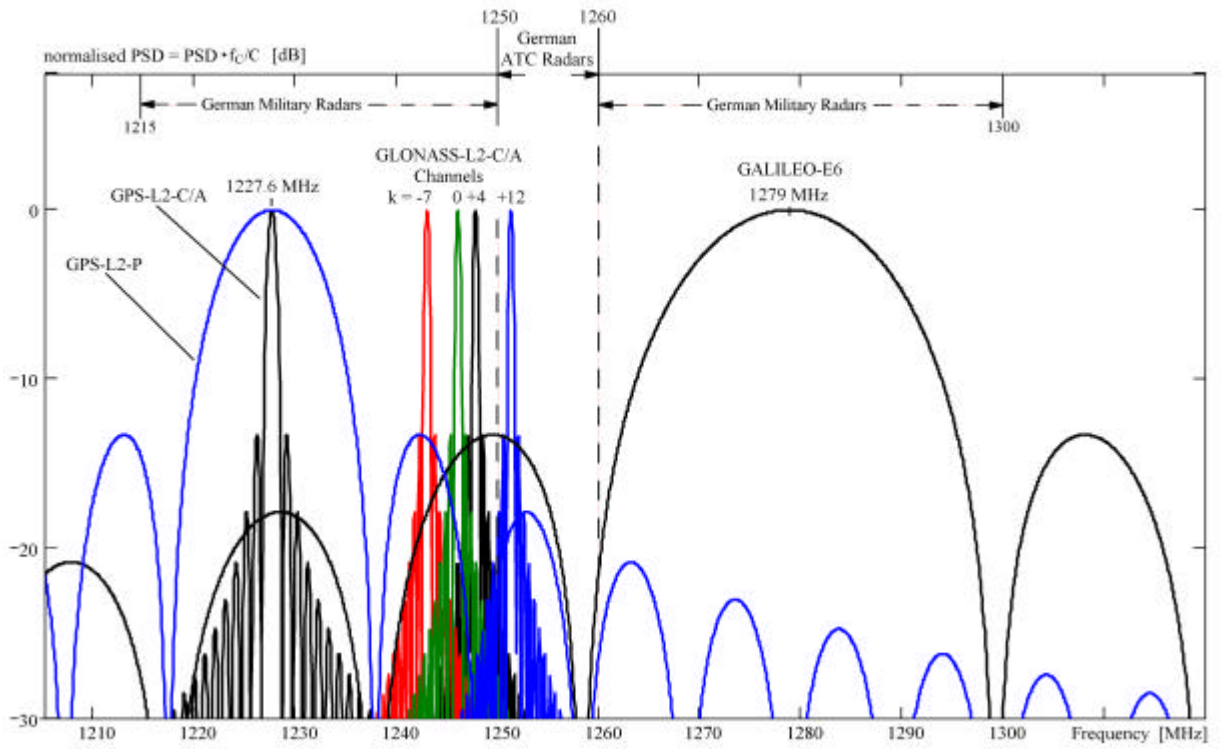


Fig. 1: Spectra of satellite navigation signals in the frequency band under consideration (1215 to 1300 MHz)

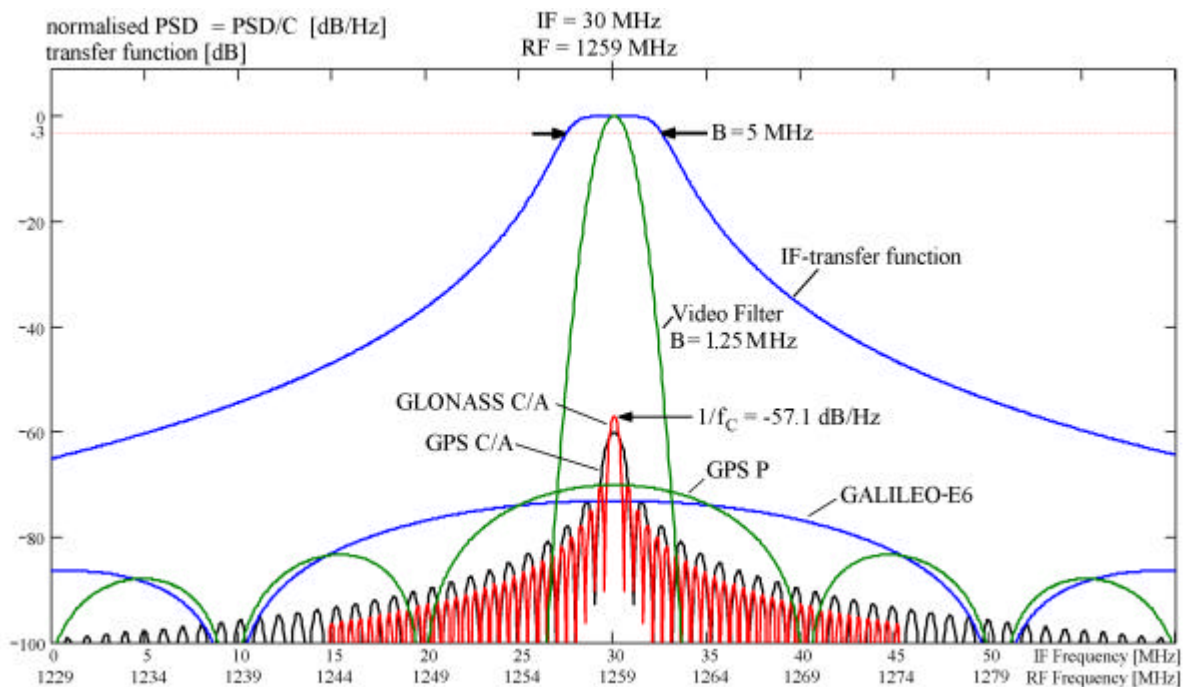


Fig. 2: Spectra of the used Interference Signals and Transfer Functions

4. RESULTS / FINDINGS

The impact of the signals were investigated as follows:

At first the spectrum of the received signals at the output of the Low Noise Amplifier as well as at the output of the IF-stage were examined in the undisturbed as well as in the disturbed case. In this way the filtering of the interference signal and the increase of the noise floor can be judged (see section 4.2). After having determined the range of values of the power levels to be used to rise the noise floor between 1 and 20 dB, the various interference signals (as described in section 3.2) were applied for one hour per each step of power level. During this time, the target reports were evaluated by means of the SASS-C software (see section 4.3).

4.1 Considerations about the Radar antenna

The figures Fig. 13, Fig. 14 and Fig. 15 (in Appendix A) present various views of the Radar's antenna pattern. The half power beam width of the azimuth cut is extremely low (1.1°). Therefore it is unlikely that the signals of more than one navigation satellite are received simultaneously and their power is aggregated. The Radar is able to switch between four different beam types (Pencil Beam, COSEC² beam, Combined Beam No. 1 and Combined Beam No.2). A so-called Range Azimuth Generator is programmed to switch between these beam types in such a way, that the received clutter is minimised. Satellite signals received by the Pencil Beam with its high gain of 38.6 dBi (at an elevation of 0.7°), pose the biggest interference threat.

4.2 Interference impact on the Radar receiver

4.2.1 Considerations about the impact of various types of interference signals

It is common to determine an interference-to-noise threshold I/N for the protection of Radars. In general, the interference-to-noise ratio within the relevant bandwidth B for interference by satellite navigation signal can be determined as follows:

$$\frac{I_B}{N_B} = \frac{\int_{f_{sat} - \frac{B}{2}}^{f_{sat} + \frac{B}{2}} PSD(f) df}{N_0 \cdot B} \quad \text{Eq. 1}$$

Where:

- PSD Power Spectral Density in dBm or dBW
- N_0 : Noise power of the radar receiver in 1 MHz
- f_{sat} : Centre frequency of the radar receiver
- N_B : Noise power within the relevant bandwidth in dBm or dBW
- I_B : Interference power within the relevant Bandwidth B in dBm or dBW
- B: index representing the bandwidth, here called reference bandwidth, e.g. B="1M" for 1 MHz and B="5M" for 5 MHz

In many existing ITU and CEPT documents about the impact of interference to Radar, the interference of a noise like signal is discussed. For noise like interference the reference bandwidth, within which the I/N is determined does not have any influence, since the power spectral densities of the interference, as well as of the noise are independent of the frequency. For the case of simplicity, often (e.g. in ITU-R.M 1463) the IF-bandwidth of the Radar (e.g. 5 MHz) is used for the calculation of the I/N.

For noise like interference an I/N of -6 dB causes theoretically an increase of the total noise power (thermal plus artificially generated by the interference signal noise) of 1 dB. The I/N ratio of -6 dB is commonly regarded as an appropriate protection limit.

It turns out that for interference signals which are not noise like, which is the case for most RNSS signals, the reference bandwidth for which the I/N is determined plays an important role. If the occupied bandwidth of the interference signal is much lower than the IF-bandwidth of the Radar, there is a strong dependence of the I/N ratio from the reference bandwidth. Actually mainly the interference power which is received within the occupied bandwidth of the Radar (e.g. 1 MHz for a Radar with 2 μ s pulse width, rather represented by the video bandwidth, than the IF bandwidth of the Radar) has an influence.

For example in the case of the GLONASS C/A signal (code chip width 2 μ s), the occupied bandwidth is in the same order (approx. 1 MHz) as the occupied bandwidth of the Radar considered in this study. On the other hand, the noise power within the IF bandwidth of 5 MHz is approx. 7 dB (Factor 5) higher, compared with the noise power within 1 MHz. At the same time, the interference power received within 5 MHz and within 1 MHz respectively, are almost the same (0.3 dB more within 5 MHz compared to 1 MHz). For this reason the I_{1M}/N_{1M} is approx. 7 dB (precisely 6.7 dB) less than the I_{5M}/N_{5M} .

For illustration of this effect Tab. 2 presents the quotients of the signal power values S_B and I_B/N_B values for reference bandwidth values of $B = 5$ MHz and 1 MHz (obtained by applying Eq. 8 and Eq. 12 in Appendix B). (A more detailed theoretical background is presented in Appendix B.)

Tab. 2: Parameters for the various satellite navigation signals

	S_{5M}/S_{1M}	N_{5M}/N_{1M}	$(I_{5M}/N_{5M}) / (I_{1M}/N_{1M})$
Signal Type	Ratio of 'signal power within 5 MHz' and 'signal power within 1 MHz'	Ratio of 'noise power within 5 MHz' and 'noise power within 1 MHz'	
GLONASS C/A	0.3 dB	7 dB	-6.7 dB
GPS C/A	0.9 dB	7 dB	-6.1 dB
GPS P	6.7 dB	7 dB	-0.3 dB
GALILEO E6	6.9 dB	7 dB	-0.1 dB

4.2.2 Considerations about potential saturation of the low noise amplifier

The 1 dB compression point of the low noise amplifier of SREM Radar is -30 dBm = -60 dBW referenced to the LNA input. The attenuation between antenna output and LNA input for the considered Radar is 5.7 dB (Appendix A, Fig. 17). Therefore, the power level of a signal at the antenna port must be 5.7 dB stronger to be able to saturate the LNA. That means, it must have a power of -54.3 dBW. The satellite navigation systems under consideration signals are much weaker.

For example, a single GLONASS satellite has a nominal signal power of -161 dBW, referenced to the output of an antenna with 0 dBi gain. If a maximum Radar antenna Gain of 38.6 dB is assumed (see Appendix A and Fig. 15), the received power of one GLONASS satellite would be -122.4 dBW. Therefore, there is a safety margin of 68.1 dB left.

4.2.3 Measured impact at the IF stage output

Fig. 3 and Fig. 4 show the spectra of a typical narrow band (GLONASS C/A) and a typical wide band (GALILEO E6) satellite navigation signal at the output of the IF stage. It is striking that the narrow GLONASS C/A signal passes the channel of the Radar near undistorted, while only the centre part of the main lobe of the broadband Galileo E6 signal can be seen at this interface. The GALILEO E6 signal behaves more similar to white noise (power spectral density constant within the bandwidth under consideration) than the GLONASS L2 signal.

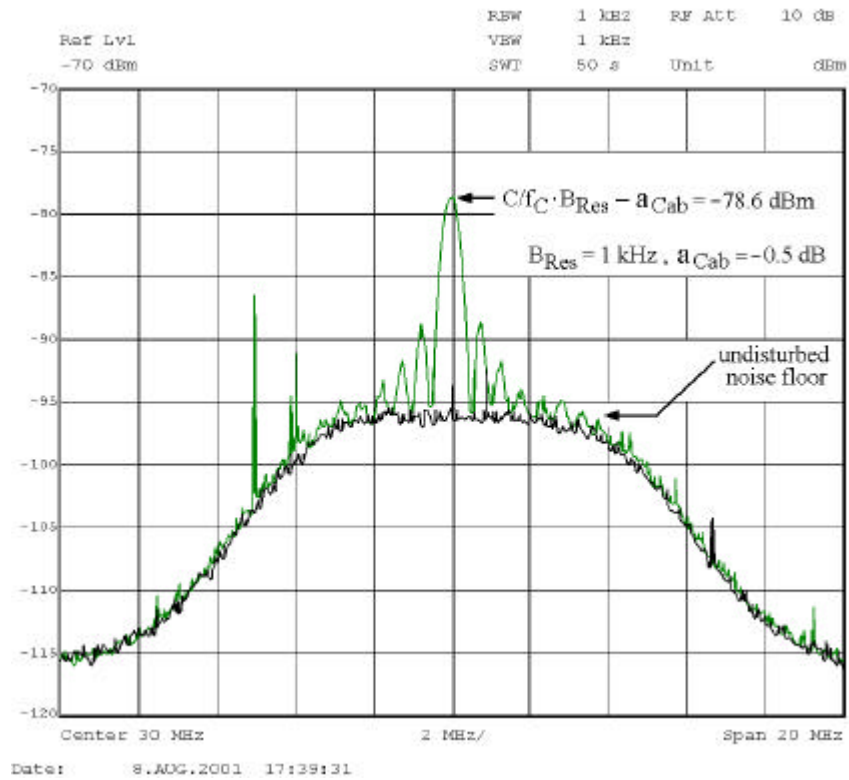


Fig. 3: GLONASS L2 C/A signal at the output of IF stage (IF = 30 MHz, resolution bandwidth 1 kHz)

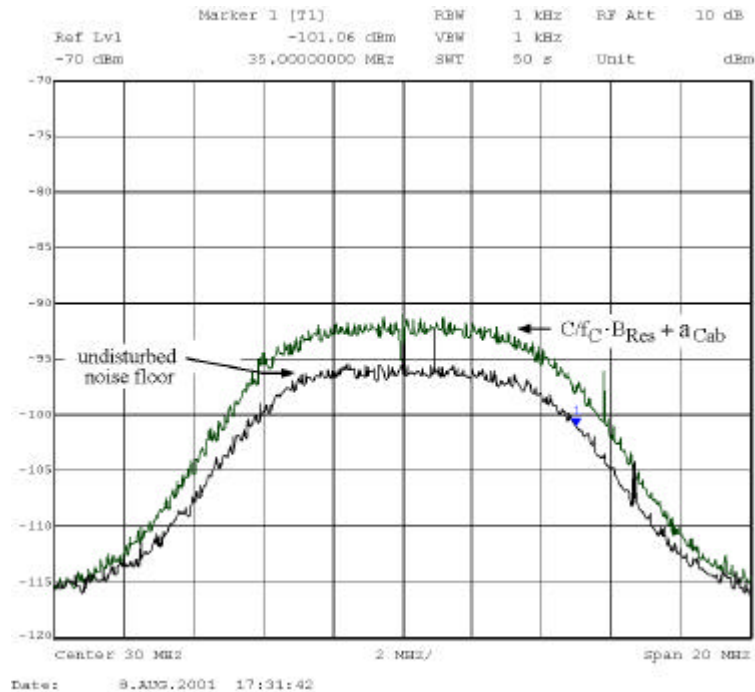


Fig. 4: Galileo E6 signal at the output of IF stage (IF = 30 MHz, resolution bandwidth 1 kHz)

The spectra depicted in Fig. 3 and Fig. 4 were measured with a resolution bandwidth of $B_{Res}=1$ kHz. The measurement cable had a loss of $a_{Cab}=-0.5$ dB. The undisturbed noise floor at the IF stage according to the Fig. 3, Fig. 4 is about -96.5 dBm/kHz = -96.5 dBW/MHz. Taken into account a insertion gain of 45.4 dB between antenna and output of the IF stage (Fig. 17), this corresponds to a noise floor referenced to the antenna output of -141.9 dBW/MHz (-111.9 dBm/MHz).

A satellite navigation signal starts to significantly increase the noise floor, if the maximum of its PSD of C/f_C (Carrier power divided by code clock frequency, see Appendix B, this corresponds to $C/f_C \cdot B_{Res}$, if measured with a spectrum analyser with a selected resolution bandwidth of B_{Res} , see Fig. 3 and Fig. 4) reaches the value of the undisturbed noise floor. With a given effective antenna are of 15.15 dBm² (Pencil beam, see Appendix A, Tab. 5), this threshold of -141.9 dBW/MHz corresponds to a PFD of approx. -157 dB(W/(m²MHz)). The Fig. 5 depicts the measured increase of the noise floor caused by a simulated GLONASS C/A signal versus its PFD value. It can be easily seen, that the noise floor starts to increase at a PFD value of -166 dB(W/(m²MHz)) and the increase reaches a value of 3 dB, as expected, at -157 dB (W/(m²MHz)).

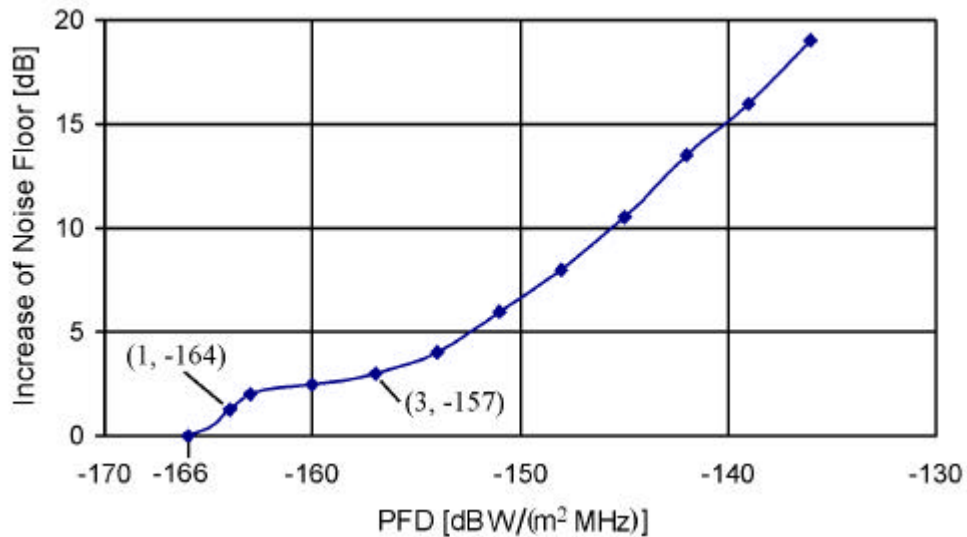


Fig. 5: Increase of the noise floor caused by a simulated GLONASS C/A signal versus its PFD value

Fig. 6 shows a plot of the Minimum discernible signal as a function of the increase of the noise floor. It is fairly obvious, that the MDS is increasing by approximately 1 dB per 1 dB increase of the noise floor level. In Fig. 5 it can be seen that at a PFD value -164 dB(W/(m²MHz)), the noise floor is increased by about 1 dB. This causes the MDS according to Fig. 6 to rise about 0.8 dB.

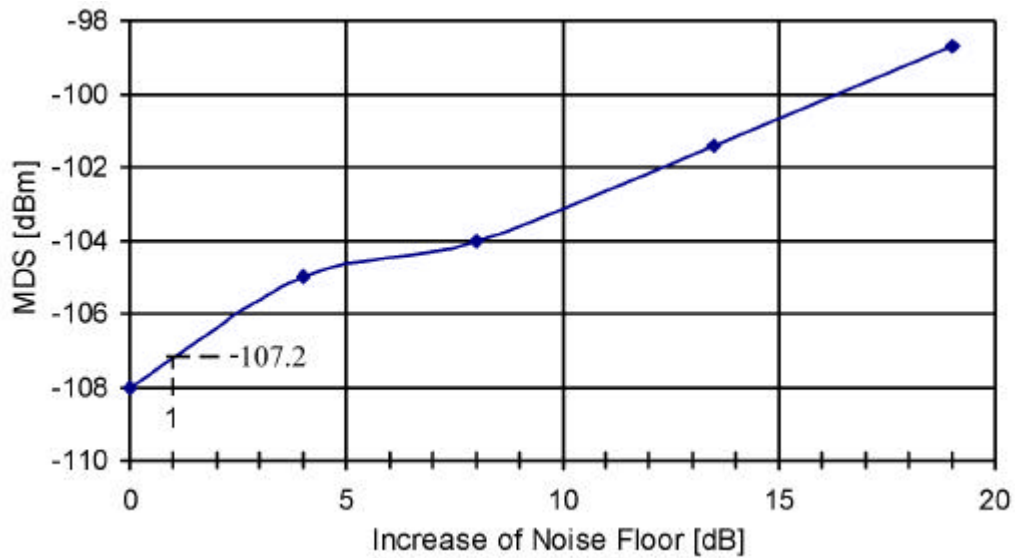


Fig. 6: MDS versus increase of noise floor

4.3 Interference impact on Radar processing

For a variety of power levels of the simulated satellite navigation signal the loss in probability of detection has been determined. To simulate the impact of a satellite navigation system realistically, it was assumed that a maximum number of 12 satellites can be received simultaneously.

The signals from these twelve satellites were expected to be received from 12 almost equally separated directions. Moreover, it was assumed, that an individual satellite is only received within an angle sector with a width corresponding to approximately twice the half power beam width of the Radar i.e. within a sector of 2° . To simulate this scenario, the signal generator was switched on by a trigger signal output by the Radar. (The measurement set-up is described in detail in Appendices A, Fig. 12).

From the power levels of the unmodulated carrier C selected at the signal generator, the corresponding PFD and I/N ratios referenced to the antenna were calculated. For this purpose, the loss values of measurement cables, wave guide sections as well as the effective area of the antenna had to be determined (see Appendix A, Fig. 12 and Fig. 17). To determine the relevant effective antenna area, the following assumption was made: Out of the four different beam types that can be selected for this Radar (Pencil Beam, COSEC² beam, Combined Beam No. 1 and Combined Beam No.2 see Fig. 14 and Fig. 15), the Pencil Beam with its maximum Gain of 38.6 dBi at an elevation angle of 0.7° has been selected as a worst case. The reason is, that a satellite signal received by the pencil beam with its high gain would have the strongest impact. Furthermore to determine the interference power I_b , within the IF bandwidth B of the Radar, the ratio of signal power within the B and the Carrier Power C was calculated (Eq. 2 in Appendix B). For the determination of the PFD the interference power within a bandwidth of 1 MHz referenced to the antenna port was divided by the effective antenna area (PFD was obtained by applying Eq. 9 and I/N by using Eq. 7 in appendix B). In order to obtain the I/N ratio, the interference power occurring within a reference bandwidth of 5 MHz (IF bandwidth of the Radar) referenced to the antenna port was divided by the theoretical noise power referenced to the same interface (obtained by applying Eq. 7 in Appendix B).

During the measurements, the power of the interference signal was increased in steps of 6 dB for the measurements. Radar data were recorded for one hour for every single signal level that was selected. From the data recorded during intervals of nearly one hour (55 minutes), the Probability of Detection (P_D), was determined within the 12 sectors with a width of 2° each, for the disturbed channel (1259 MHz), as well as for the undisturbed channel (1343 MHz) using the SASS-C software. The difference of the P_D between these two channels was regarded as the loss of P_D caused by the interference signal.

It should be mentioned, that received echoes were rather produced by big aircraft with Radar cross sections greater than the reference value of 4 m^2 , for which the performance of the Radar is specified (Appendix A Tab. 5). The value of the P_D loss was normalised to the P_D of the undisturbed channel.

GLONASS C/A and GPS C/A are the signals with the most severe impact. It can be seen in Fig. 7 that for GLONASS C/A the P_D starts to degrade significantly at PFD values in the order of $-154 \text{ dB(W/(m}^2\text{MHz))}$. In the same figure for the GPS C/A signal the P_D starts to degrade significantly already at PFD values in the order of $-164 \text{ dB(W/(m}^2\text{MHz))}$.

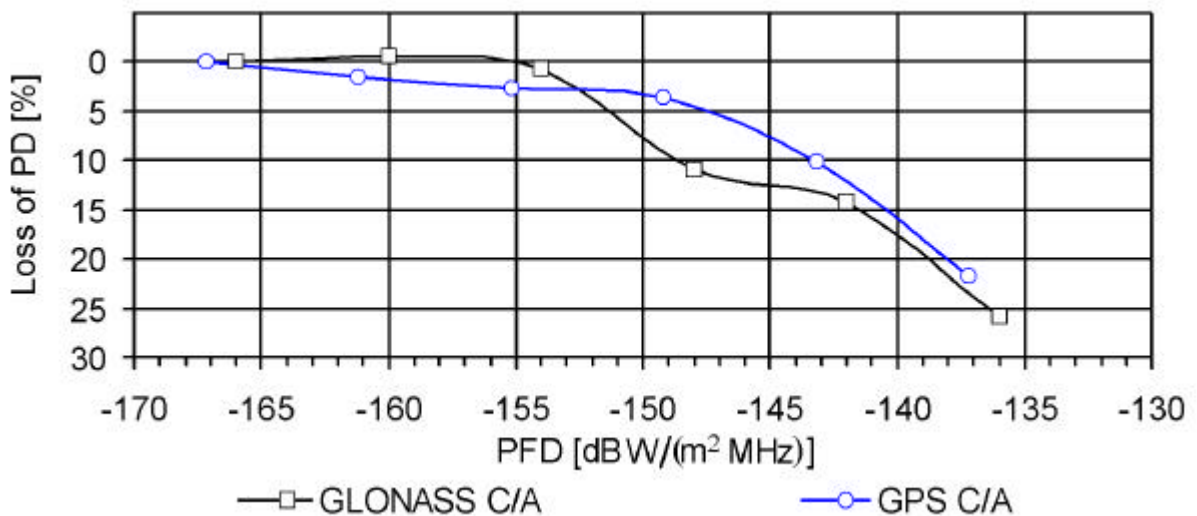


Fig. 7: Loss of P_D versus PFD for GLONASS C/A and GPS C/A

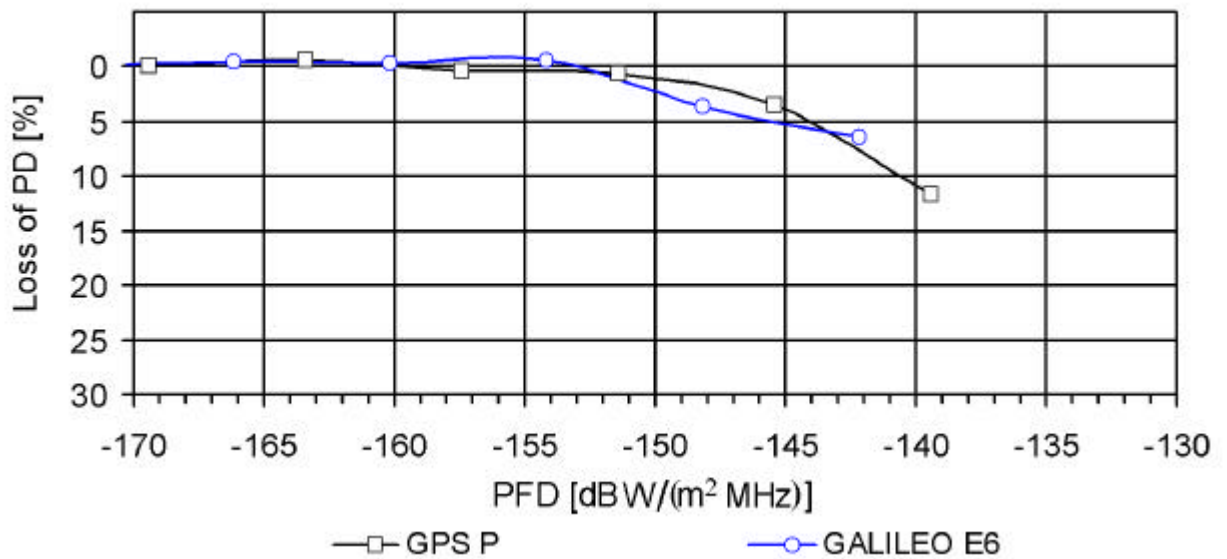


Fig. 8: Loss of PD vs. PFD for GPS P and GALILEO E6

In Fig. 9 and Fig. 10 of the loss of Probability of Detection (PD) as a function of the I/N ratio (the I/N ratio referenced to a bandwidth of 5 MHz I5/N5) is depicted for the various signals., The PD starts already to degrade at an I/N ratios of -11 dB for GLONASS C/A and -18 dB for GPS C/A. For GPS/P and GALILEO E6, the PD starts to degrade not below -3 dB.

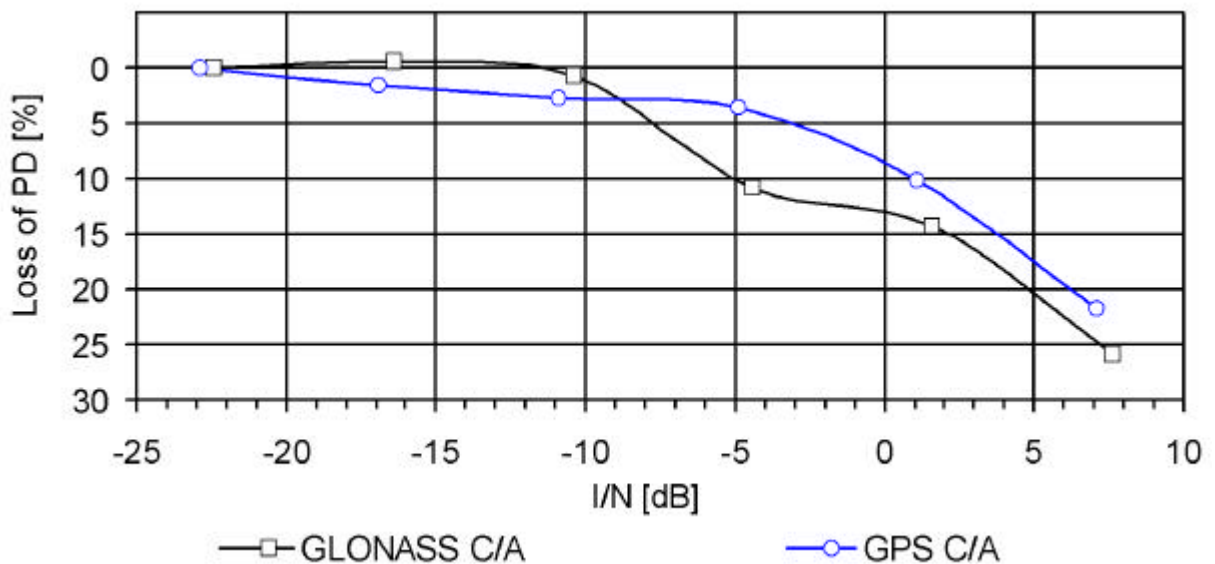


Fig. 9: Loss of P_D versus I/N for GLONASS C/A and GPS C/A

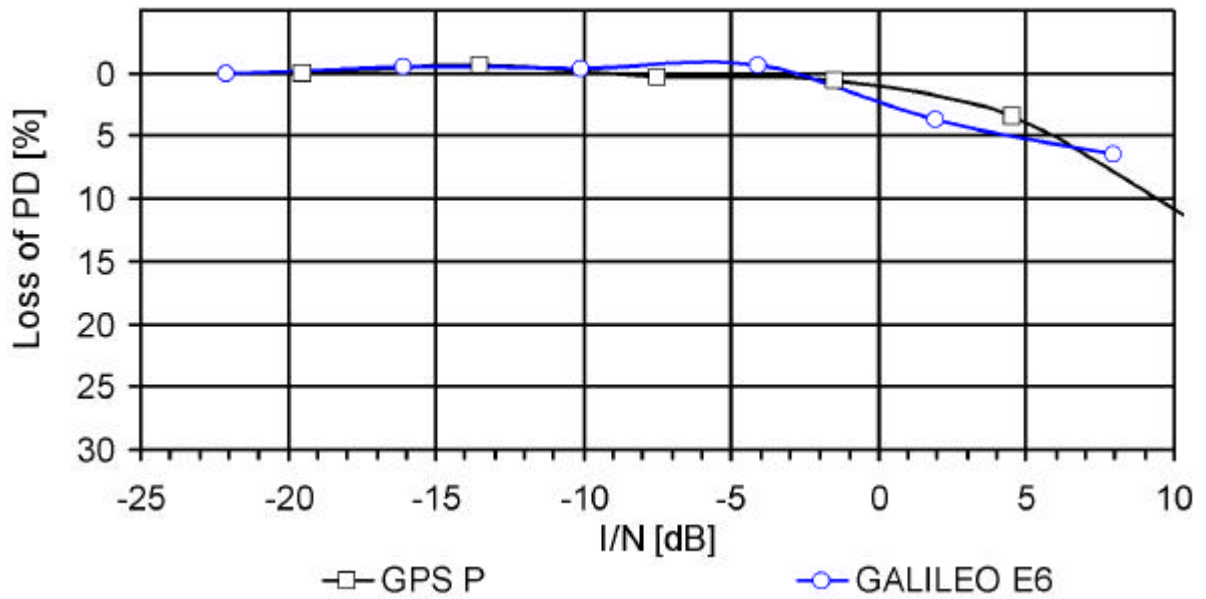


Fig. 10: Loss of P_D vs. I/N for GPS P and GALILEO E6

Tab. 3: Measured interference thresholds

Signal Type	I/N (5 MHz BW)	I/N (1 MHz BW)	$(I_{1M}/N_{1M}) / (I_{5M}/N_{5M})$
GLONASS C/A	-11dB	-4.3 dB	6.7 dB
GPS C/A	-18 dB	-11.1 dB	6.1 dB
GPS P	-3 dB	-2.7 dB	0.3 dB
GALILEO E6	-3 dB	-2.9 dB	0.1 dB

Signal Type	PFD-Threshold
GLONASS C/A	-154 dB(W/(m ² MHz))
GPS C/A	-164 dB(W/(m ² MHz))
GPS P	-151 dB(W/(m ² MHz))
GALILEO E6	-151 dB(W/(m ² MHz))

Tab. 3 summarises the measured I/N limits. These limits would keep the loss of P_D below 1 % and the increase of noise as well as the increase of the minimum discernible signal level below 1dB. It turned out, that the I/N limit does depend very much on the reference bandwidth, since narrow-band RNSS signals can not be considered as noise like compared with the IF bandwidth of the Radar.

This is due to the fact, that the reference bandwidth is higher than the occupied bandwidth of the interference signal. Thus the noise power is overestimated compared to the interference power. Values for I/N limits determined in this way, appear to be unusual, but are not incorrect, as long as the reference bandwidth used to determine these values is mentioned. It should also be noted that the I/N ratios obtained for a reference bandwidth of 1 MHz (I_{1M}/N_{1M}), are closer to the Radar protection limits of $I_{5M}/N_{5M} = I_{1M}/N_{1M} = -6$ dB as developed by ITU-R for noise like interference than the I_{5M}/N_{5M} values.

Concerning the impact of the simulated interference signals on the Probability of False Alarm, P_{FA} , the following has been found out: Interference signals exceeding the interference threshold caused false targets at the raw video display (Fig. 19). But the tracking software was able to eliminate nearly every single one. To appear as a valid target a potential target has to appear at 5 revolutions of the antenna and has to fit into a track. This condition can not be fulfilled by a noise-like interference signal.

According to ITU Doc 8D/18 [Ref. 4], the maximum PFD per satellite is for a GLONASS C/A code signal -133.3 dB(W/(m²·MHz)) and -142.2 dB(W/(m²·MHz)) for GPS P signal. The results in Fig. 7 and Fig. 8 suggest a considerable impact due to such signals on Radars operating at the same centre frequency. According to Fig. 7 a loss of P_D of 20 to 30 % for GLONASS C/A and according to Fig. 8 a loss of PD of 5 to 15 % for GPS P, could be expected. This loss is only caused within angle sectors, where a navigation satellite is received.

4.4 Interference conditions in Germany

From the measurement results describe in section 4.3, it could be concluded that the signals transmitted by existing satellite navigation systems have an impact on Radars. Nevertheless, in Germany such an impact has not been detected in the past. As mentioned above, the German L-band ATC Radars are within the band 1250 to 1260 MHz. As it can be seen from Fig. 1, and Tab. 4 only the signals of the GLONASS satellites 10, 11 and 12 are within the band 1250 to 1260 MHz. Only one of these satellites, namely satellite No. 10 was during the year 2001 active. Tab. 4 contains the list for the centre frequencies of the six German ATC Radars in this band. Only the Radar "Schmooksberg", one of six German ATC Radars in this band with a centre frequency of 1251 MHz could be affected by GLONASS (Tab. 4). A comparison of the spectrum of the GLONASS channel 10 with the IF transfer function of the Radar "Schmooksberg" (Fig. 11) shows, that the spectrum is not centred with the Radar channel. This GLONASS signal is not suppressed by an IF-filter transfer function (depicted in Fig. 11), but should be partly suppressed by the video filter. Unfortunately the Radar "Schmooksberg" was not available for measurements described in this study.

In the past there was no impact by GLONASS on this Radar detected. This could be for several reasons:

- Only a narrow angle segment with a width of 1° to 2°, is potentially affected;
- People responsible for this radar were not aware of the problem;
- The number of satellites transmitting co-frequency is very limited.

It is obvious, that the situation will become more severe, the moment GLONASS satellites using the channels 11 and 12 will be used again (Satellite 12 was launched in December 2001). On the other hand, after the year 2005, GLONASS will not use any more the channels 8 to 12. This will improve the situation for the German ATC Radars.

Tab. 4: Frequency list of German L-band ATC Radars and list of GLONASS L2 channels

Frequency List of German ATC Radars		Centre frequencies of GLONASS L2 channels	
Name of the Radar station	Frequency	Channel No. K	L2-Frequency [MHz]
Schmooksberg	1251 MHz	-7	1242.938
Nordholz	1253 MHz	-6	1243.375
Auersberg	1253 MHz	-5	1243.813
Neunkircher Höhe	1257 MHz	-4	1244.250
Deister	1259 MHz	-3	1244.688
Grosshaager Forst	1259 MHz	-2	1245.125
		-1	1245.563
		0	1246.000
		1	1246.438
		2	1246.875
		3	1247.313
		4	1247.750
		5	1248.188
		6	1248.625
		7	1249.063
		8	1249.500
		9	1249.938
		10	1250.375
		11	1250.813
		12	1251.250

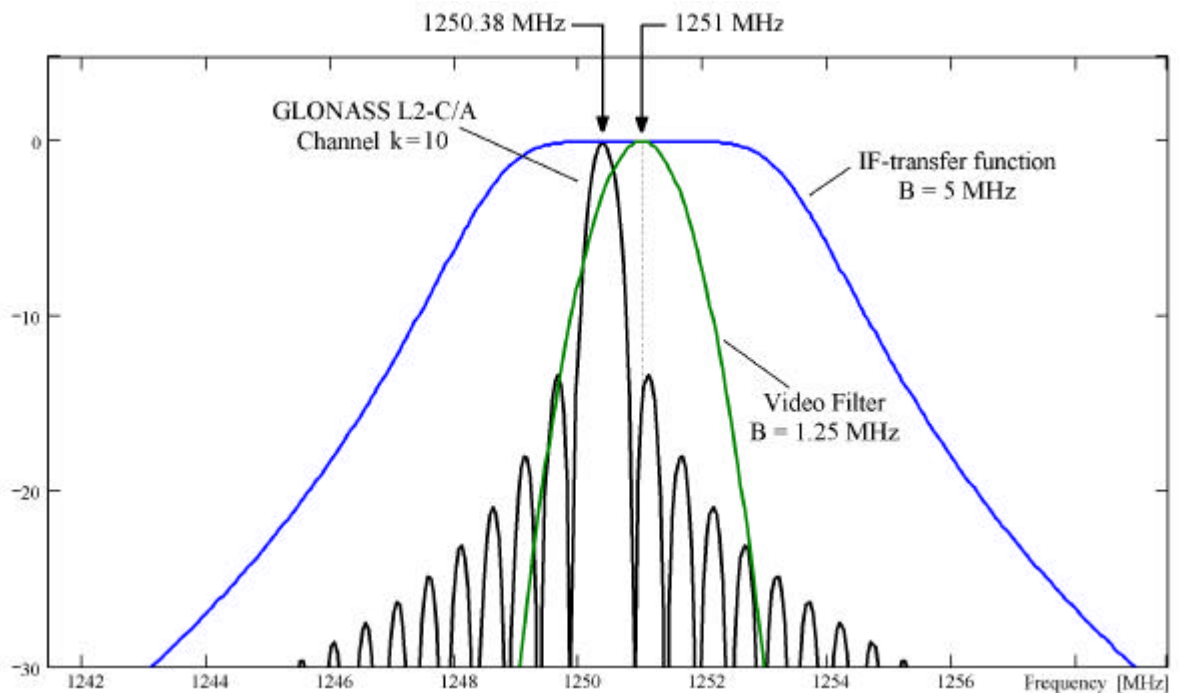


Fig. 11: Comparison of GLONASS channel k=10 and Radar channel at 1251 MHz

5. CONCLUSION / RECOMMENDATIONS

Preliminary theoretical evaluation of the maximal RNSS Power Flux Density (PFD) to protect L-band Radar has been presented to ITU, CEPT and ICAO. The theoretical PFD value was derived from the radar interference protection limit as stipulated by ITU-R Recommendation M.1461 for the worst case scenario where the satellite transceiver is in the same azimuth than the aircraft target and when the central frequency of the satellite transceiver and of the radar receiver is the same.

The purpose of this study was to provide more experimental material to confirm the theoretical calculations derived from the ITU-R Recommendation M.1461.

Measurements have been conducted to determine the sensitivity to RNSS signals of ATC Radar operated by the German Air Navigation Services DFS at a carrier frequency of 1259 MHz. The simulated RNSS signals were centred at 1259 MHz and injected at the input of the low noise amplifier of the radar receiver, with the antenna rotating and at specific times corresponding to 12 selected azimuth directions with the highest observed air-traffic density. The impact of the simulated RNSS interference signals was investigated primarily by determination of the loss of the probability of detection (P_D) of targets, - compared with the second undisturbed channel of the radar at 1343 MHz. The probability of detection was assessed using the EUROCONTROL SASS-C software tool which reconstructs individual aircraft trajectories by chaining and smoothing individual plots, extracted after each radar scan. Comparison of the position and presence of those plots with their associated trajectory allows counting the number of hits and misses from which P_D is derived.

The results of the interference susceptibility measurements show that the reduction in the probability of detection of the radar is observably degraded at I/N ratios of between -4 and -11 dB (1 MHz reference bandwidth) for narrow-band RNSS signals, and for wide-band RNSS signals the corresponding I/N ratio is -3 dB (1 MHz reference bandwidth). These limits would keep the loss of P_D below 1 % and the increase of noise as well as the increase of the minimum discernible signal level below 1 dB. The measured I/N ratios correspond to pfd values of between -154 and -164 dB(W/m²) in any 1 MHz for narrow-band RNSS signals and of -151 dB(W/m²) in any 1 MHz for wide-band RNSS signals respectively.

German civil ATC Radars utilise carrier frequencies in the band 1250 to 1260 MHz. Within this band, at the time of the study (August – September 2001), the only satellite navigation signal that could be received, was transmitted by a GLONASS satellite with the channel number 10. Despite the fact, that the measurements with simulated RNSS signals have shown a loss of probability of detection up to 25 % in the direction of the satellite transmitter, an impact was not reported in the past. The reasons for this might be, that people responsible for this radar system were not aware of the problem, that only one RNSS satellite was transmitting near the radar carrier frequency, and that only a narrow angle segment with a width of 1° to 2°, is potentially affected.

The measurements confirm the I/N ratio limit as per ITU-R Recommendation M.1463 derived by applying the methodology given in the ITU-R recommendation M.1461 to protect radar from wide-band noise like signals for the worst case scenario. For the RNSS narrow-

band signals which are not accounted for in the above mentioned ITU-R Recommendations, the measurements indicate an I/N ratio more stringent than for the wide-band signals. The Pfd value derived from the measurement on the worst case scenario shall be considered indicative. Further work is needed to determine the probability of occurrence of the worst case scenario where the satellite transceiver is in the same azimuth than the aircraft target and to determine the impact on the complete radar chain in order to document and quantify the potential risk on ATC operations.

6. REFERENCES

- [Ref. 1] „Assessment of the interference from RNSS into Radars in the 1215 –1300 MHz Band“, ITU Doc 8B/64-E/8D/93-E, 14 th of May 2001
- [Ref. 2] “Protection of ATC-Radars operating in the Band 1215 – 1300 MHz from Emissions of Space Stations in the Radio navigation-Satellite Service”, SPG 13-14, (EUROCONTROL)
- [Ref. 3] “Study on 2700 MHz – 2900 MHz frequency band sharing between existing Aeronautical Radar Equipment and planned Digital ENG/OB and Digital Aeronautical Telemetry Services”, W. L. Randeu, H. Schreiber, Technical University of Graz, May 2001. (EUROCONTROL)
- [Ref. 4] “RNSS characteristic in the band 1215 to 1300 MHz”, ITU Doc 8D/18-E, 10 th of October 2000
- [Ref. 5] “Procedures for determining the potential for interference between Radars operating in the Radio Determination Service and systems in other services“ ITU-R M.1461.
- [Ref. 6] “Characteristics of and protection criteria for Radars operating in the Radio Determination Service in the Frequency Band 1215 – 1400 MHz”, ITU-R M.1463.
- [Ref. 7] “Considerations for sharing with systems of other services operating in the bands allocated to the Radionavigation Satellite Service (GPS , ITU-R M.1088, 1994
- [Ref. 8] “Considerations for sharing between systems of other services operating in the bands allocated to the Radionavigation Satellite and Aeronautical Radio Navigation Services and the Global Navigation Satellite System (GLONASS-M), ITU-R M.1317, 1997
- [Ref. 9] „Final Acts of World Radio Conference WRC-2000“, International Telecommunication Union, Geneva, 2000
- [Ref.10] "EUROCONTROL Standard Document for Radar Surveillance in En-Route Airspace and Major Terminal Areas Ed 1.0 (SUR.ETI.1000-STD-01-01)"

APPENDIX A – DESCRIPTION OF RADAR AND MEASUREMENT SET-UP

The type of the Radar that was used for the test is called SREM (Surveillance Radar Equipment Medium range). The Tab. 5 presents the technical properties of such a Radar.

Tab. 5: Technical Data of the SREM Radar

Type of Radar		SREM (upgraded SRE-M5)
Two channels		2 centre frequencies in the frequency range 1250 to 1350 MHz 41, or 67 or 78 MHz separated
(Grosshaager Forst)		(1259 MHz /1343 MHz)
Pulse duration		2 μ s
Pulse repetition frequency		320 to 475 Hz
Maximum range		143 NM, with RCS of 4 m ² , $P_D \geq 80 \%$, $P_{FA} = 10^{-6}$
Transmitter:		
Transmitter manufacturer / type		DASA / SREM
Transmitter technology		Klystron
Transmitter peak power		2.5 MW
Antenna:		
4 Beams: Pencil, Cosec ² , Combined No. 1, Combined No. 2:		
Combined beam No.1 (transmit beam)		35.6 dB
Pencil beam		38.6 dB
=> effective antenna area (Pencil Beam)		15.15 dBm ²
Cosec ² beam		34.3 dB
Combined beam No.2		35.0 dB
Tilt		1.7° mechanical tilt
Azimuth 3 dB width		1.1°
Cone of silence		107.8°
Antenna rotation		5.157 rpm => 11.635 sec / rotation
Polarisation		vertical / circular
Receiver:		
Receiver manufacturer / type		Alenia / TWRPM (Target and Weather Receiver and Processor)
Intermediate frequency		30 MHz
Receiver noise figure		9 dB
HF-receiver bandwidth:	-3 dB	10 MHz
IF-Receiver bandwidth :	-3 dB	4.9 MHz
	-40 dB	40 MHz

Video Filter Type		Gaussian
Video Bandwidth	-3 dB	1.25 MHz
Noise Power within IF bandwidth		-98 dBm
Minimum Discernible signal, MDS		-108 dBm
Sensitivity Time Control (STC)		0 to 63.5 dB attenuation in 0.5 dB steps
Low Noise Amplifier (LNA), Gain		36 dB
LNA, Noise Figure		1.8 dB
LNA, 1 dB compression		-30 dBm at LNA input
1 dB compression, referenced to antenna output		-24.3 dBm = -54.3 dBW
Typical insertion loss between antenna output and LNA input (Grosshaager Forst)		5.7 dB
Typical insertion gain between antenna output and IF output (Grosshaager Forst)		45.4 dB
Nominal Probability of detection (P_D)		≥ 80
Nominal False Alarm Rate (CFAR)		10^{-6}
Type of Doppler processing		MTD Filter Bank with 6 or 8 channels, depending on selected PRF
Angle accuracy / resolution (S/N = 10 dB)		$2^\circ / 0.16^\circ$
Range accuracy / resolution (S/N = 10 dB)		80 m / 463 m

Radars of this type have an antenna with two exciters which are connected with two different channels per frequency. One exciter has, in combination with the reflector a COSEC² antenna diagram, while the other has a pencil-shaped diagram. The exciters are connected to two different signal channels per frequency. These two channels are inter-connected two times: just after the antenna by a fixed combiner (K1, in Fig. 12) and a second time by a controllable so-called beam-combiner (K2 in Fig. 12). In combination with an individual phase shifter in front of each combiner, it is possible to switch between the COSEC² antenna diagram, the pencil diagram and two combined diagrams (Fig. 14). To select one of these four Diagrams, four different values can be selected for the phase offset of the second phase shifter φ_2 and coupling factor K2 of the second combiner (beam combiner) (Tab. 6). This fact makes it difficult to determine the insertion loss between antenna and LNA input, here called wave guide loss a_{WG} .

Tab. 6: States of the phase shifters and beam combiners necessary to select a special antenna beam

K1	φ_1	K2	φ_2	Selected Beam
$\frac{1}{4}$	-90°	$\frac{1}{4}$	180°	COSEC ² Beam
$\frac{1}{4}$	-90°	0	arbitrary	Combined 1, Transmit
$\frac{1}{4}$	-90°	adjustable	adjustable	Combined 2
$\frac{1}{4}$	-90°	$\frac{3}{4}$	0°	Pencil Beam

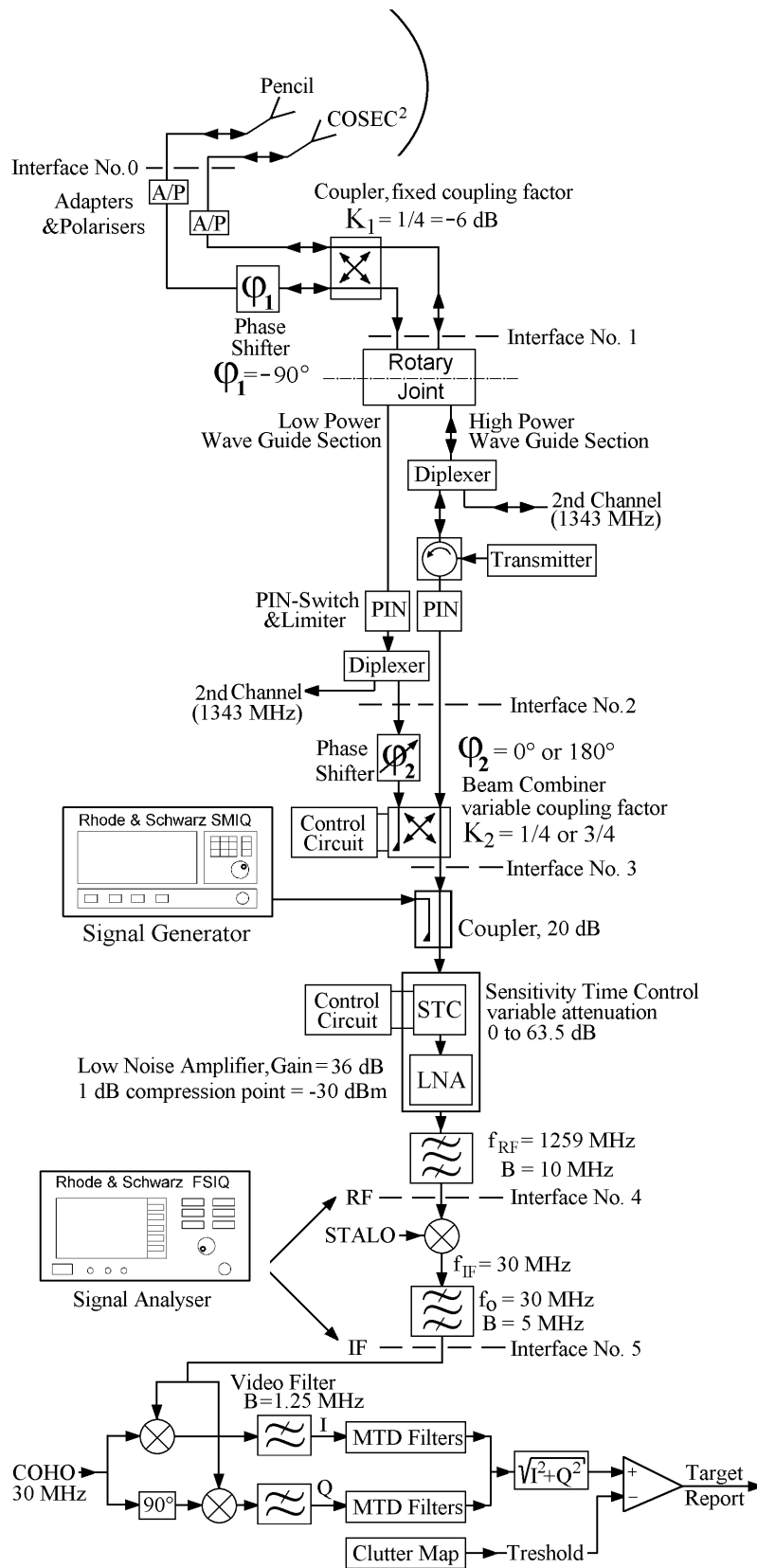


Fig. 12: Block diagram of the Radar and measurement set-up

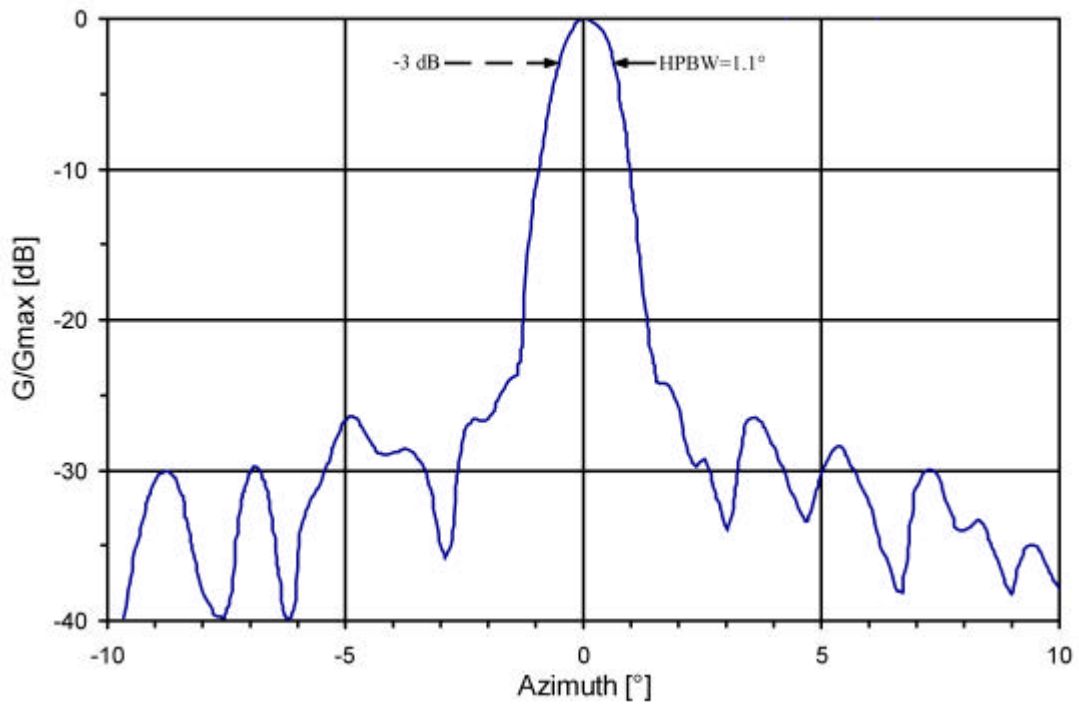


Fig. 13: Azimuth cut of the antenna diagram of the Radar

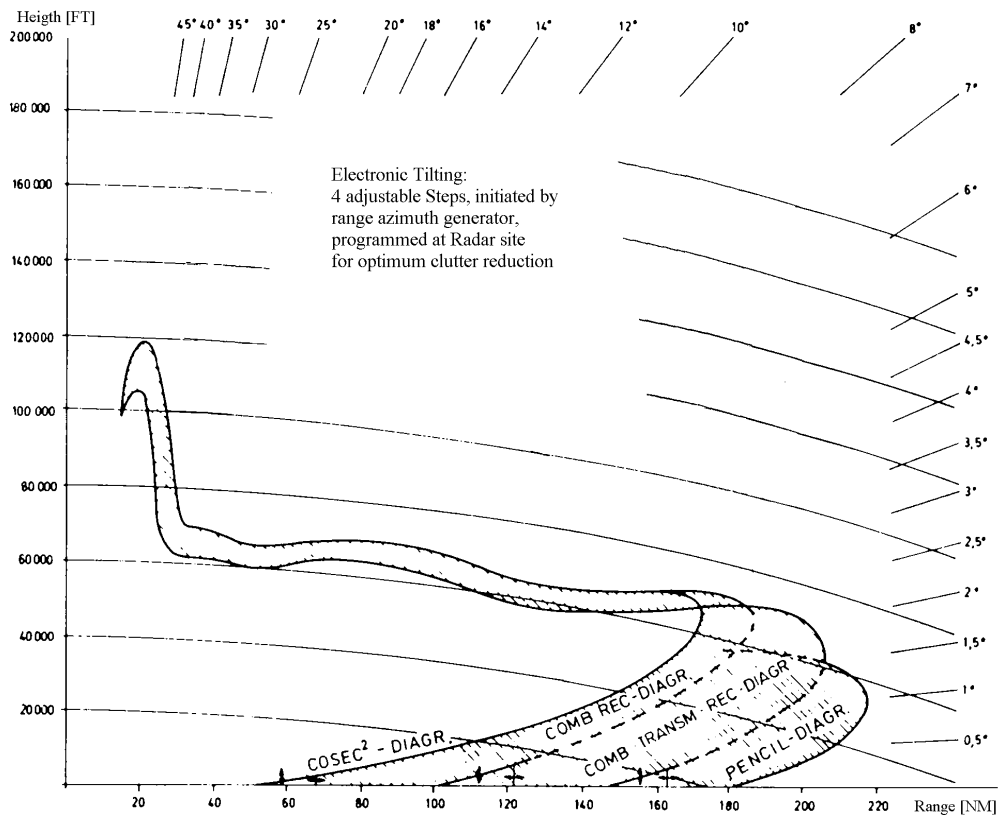


Fig. 14: Coverage Diagram (only for illustration purpose)

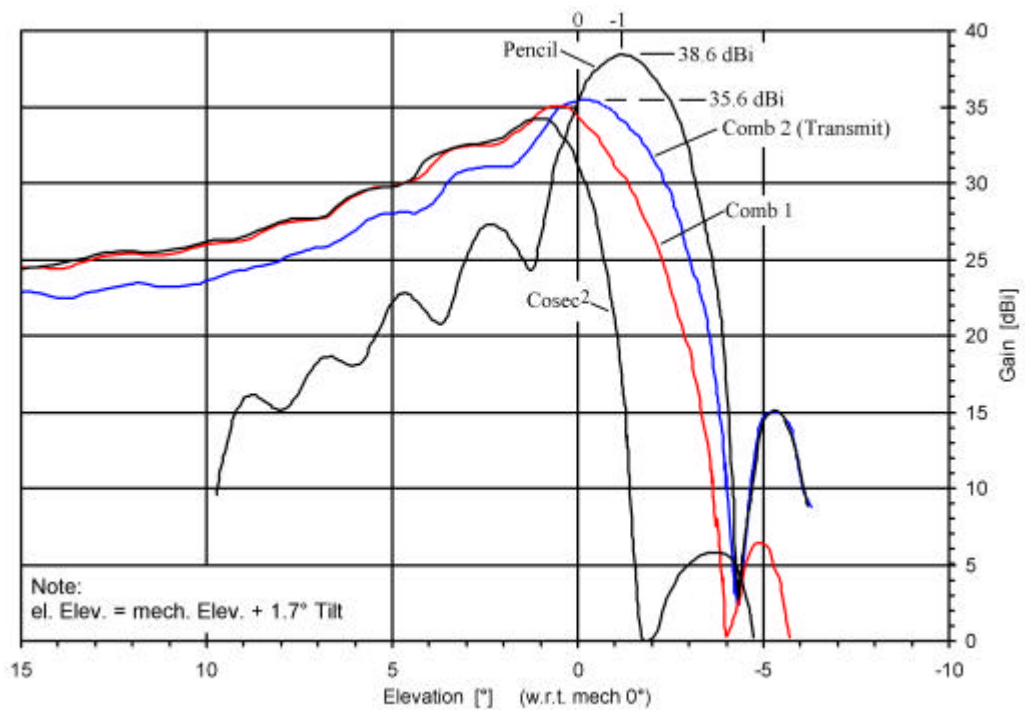


Fig. 15: Elevation cut through the four different antenna diagrams of the Radar

The Fig. 16 shows a diagram of the measured transfer function between the LNA input and the output of the IF-stage. It can be well simulated by a Butterworth filter of the order 3 with a bandwidth of 5 MHz.

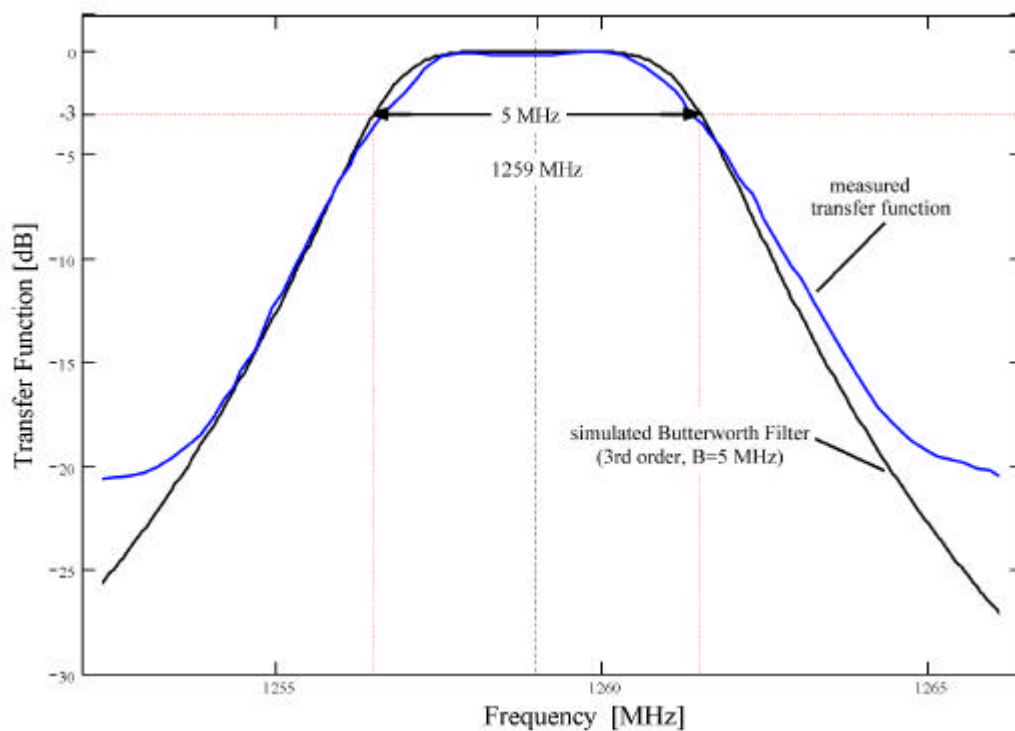


Fig. 16: Measured and simulated transfer function of the tested Radar

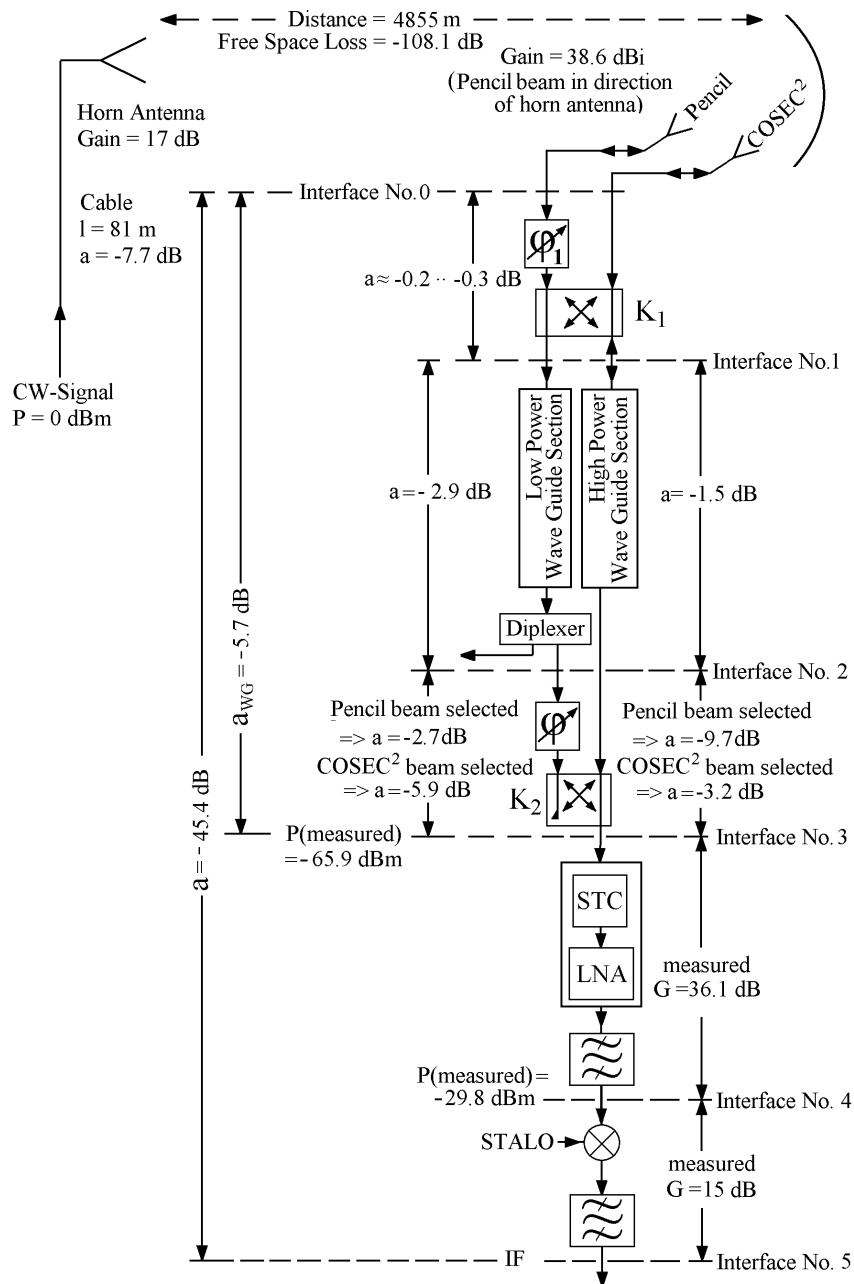


Fig. 17: Determination of the relevant attenuation values

The interference signal is fed into the signal path by means of a 20 dB coupler in front of the low noise amplifier Fig. 12. To be able to calculate the Power Flux Density (PFD) at the antenna, great care has been taken to determine the insertion loss of the signal path between antenna and the input of the LNA (a_{WG}). As described above, signals received by the antenna through two different signal paths, a high power section and a low power section and are coupled together at two different locations (combiner K1 and combiner K2). Moreover, the coupling factor of the second coupler is switchable.

Fortunately the value of a_{WG} needs to be determined only for the case when the pencil beam is selected, since the pencil beam has the highest gain and therefore represents the worst case for an interference scenario. In this case the attenuation between the low power section input and the output of the beam combiner ($K2 = -2.7$ dB) is much lower than the attenuation between high power section input and the output of the beam combiner ($K2 = -9.7$ dB).

The attenuation values measured for the individual sections of the signal paths between antenna and LNA have been taken into account to determine the total insertion loss a_{WG} . For the short wave guide section between the first combiner (K1) and the antenna horns an assessment of 0.2 to 0.3 dB loss was made. In this way a total value for a_{WG} of -5.7 dB could be determined. This value has been checked by measuring the received power level of a test signal transmitted from the location of a test transponder approx. 4.8 km apart at the LNA input (see Fig. 17).

The satellite navigation signals are simulated by modulating a pseudo noise code with suitable code clock frequency onto a carrier. The type of modulation that is used is binary phase shift keying (BPSK). The signal generator that was used is SMIQ from Rhode & Schwarz in combination with the IQ-Modulator AMIQ.

This device allows to download a pseudo noise code sequence that has been generated previously with the associated software.

The signals of the individual satellites can only be received while the main beam of the Radar sweeps across the satellite under consideration. To take this into account, the following scenario has been assumed:

- Satellite signals are only received while the main lobe of the Radar antenna with a half power beam width of approx. 2° sweeps across the satellite position
- A maximum number of 12 simultaneously received satellites is assumed

To simulate this scenario, a trigger signal for the signal generator has been generated by means of the definition of maps describing sectors with a width of 2° for 12 directions. These directions are selected in such a way that high traffic can be expected in the according sector (Radar performance monitor in display Fig. 18). The trigger signal is used to switch the interference signal coming from signal generator "on" an "off".

To check that this triggering of the interference signal is working correctly, the interference power level of a simulated GLONASS C/A signal has been set to a very high value to cause false targets and the target plot has been evaluated. Fig. 19 shows the false targets caused by a simulated interference signal with a power level corresponding to a PFD value of -136 dB(W/(m²MHz)). Which corresponds to an I/N ratio of $+7.6$ dB.

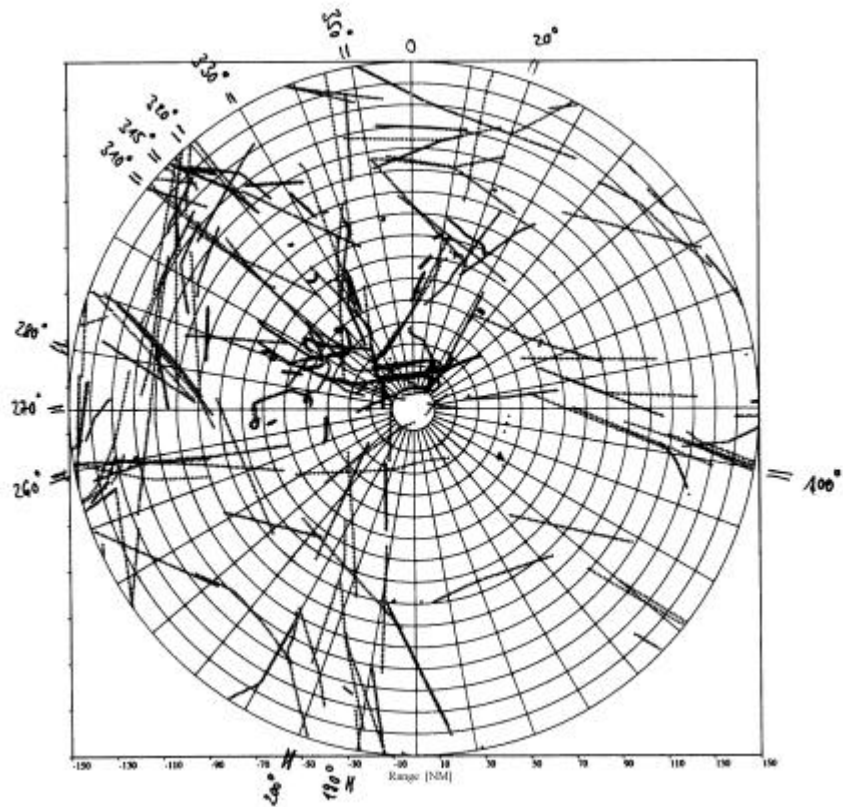


Fig. 18: Selected directions with high traffic

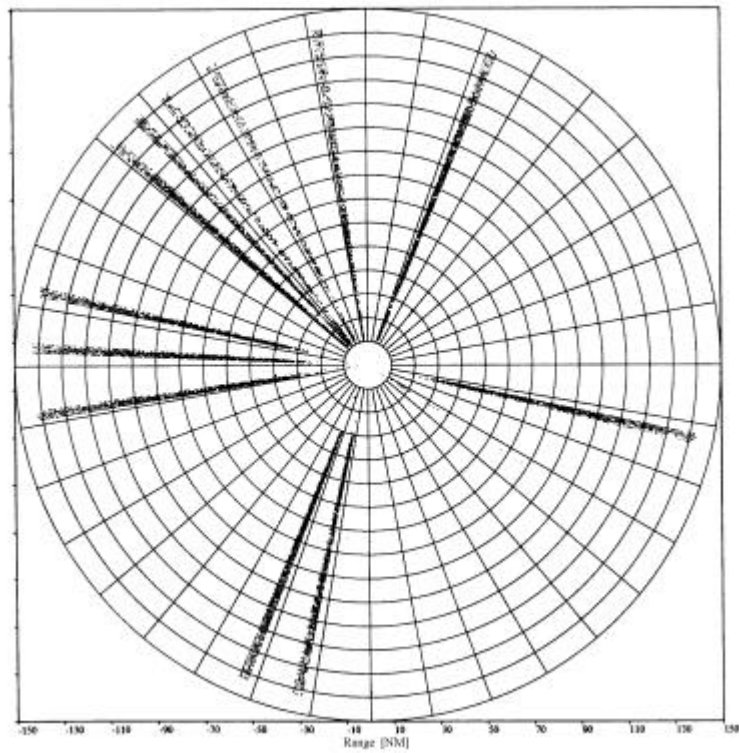


Fig. 19: False targets, caused by the simulated interference signal (PF_D = -136 dB(W/(m²MHz)))

APPENDIX B – THEORETICAL BACKGROUND

The Power Spectral Density (PSD) of a satellite navigation signal, i.e. a carrier which is being binary phase modulated with a pseudo noise code can be described as follows:

$$PSD(f) \approx \frac{C}{f_c} \cdot SINC^2\left(\frac{P}{f_c}(f - f_{Sat})\right) \quad [W/Hz] \quad \text{Eq. 2}$$

With:

C: Power of the unmodulated carrier in W, equivalent to the integral of the PSD over all frequencies

f_c : code clock frequency in Hz (e.g. 1.023 MHz in the case of GPS C/A code)

f_{Sat} : Centre frequency of the satellite signal

(Note: Eq. 2 is not valid for other modulation schemes that are also in discussion for GALILEO, like raised cosine BPSK or Binary Offset Carrier (BOC)).

Within a bandwidth B very smaller than the distance between the first minima of the PSD (i.e. $B \ll 2 \cdot f_c$) according to Eq. 2, such a signal appears as white noise with a spectral density I_b corresponding to the maximum of the PSD:

$$I_o = PSD(f = f_{Sat}) \approx \frac{C}{f_c} \quad [W/Hz] \quad \text{Eq. 3}$$

With:

I_b : equivalent noise power density in W/Hz

The interference power I_B of a satellite navigation signal received within the bandwidth of a Radar B can be described as follows:

$$I_B = C + a_{Cable} + a_{Comb} + (S_B/C) - a_{WG} \quad \text{Eq. 4}$$

With:

I_B : Interference power within the IF-Bandwidth (e.g. B = 5 MHz), in dBm or dBW

C: Power of the unmodulated carrier of the signal at the signal generator, in dBm or dBW

a_{Cable} : Attenuation of the cable between signal generator and the combiner used to feed in the signal in the Radar in dB

a_{Comb} : Coupling factor of the combiner in dB (e.g. -20 dB)

a_{WG} : Wave Guide; loss of signal path between antenna and input of Low Noise Amplifier (e.g. 5.7 dB)

S_B/C : Quotient of the signal power within the IF-bandwidth (e.g. B = 5 MHz) and the carrier power in dB. This value is important to determine how much of the power generated by the signal generator is received within the IF-bandwidth of the Radar (values for the various signal types see Tab. 7)

Where:

$$S_B/C = \frac{\int_{f_{Sat}-\frac{B}{2}}^{f_{Sat}+\frac{B}{2}} PSD(f) df}{C} \quad \text{Eq. 5}$$

The noise power within the bandwidth B can be assessed according to ITU-R.M1461 [Ref.1] as follows:

$$N_B = N_o (290K) + B + F_{Noise} \quad \text{Eq. 6}$$

With:

- N_B : Noise power within the Bandwidth B (e.g. $B = 5$ MHz), in dBm or dBW
- N_o : Noise power within the 1 Hz at room temperature in dBm or dBW (e.g. -174 dBm/Hz corresponds to -144 dBm/kHz)
- B : Bandwidth in Hz
- F_{noise} : System Noise Figure, 9 dB for the SREM Radar (Tab. 5)

(Eq. 6 corresponds to $N = -144$ dBm/kHz + $10 \log B/\text{kHz} + F_{noise}$ as used in Section 2.2.1 of Annex 1 of ITU-R.M1461 [Ref.1].)

With a value for N_o of -174 dBm/Hz and $B = 5$ MHz, and a Noise Figure F_{Noise} of 9 dB, a noise power value of $N_B = -98$ dBm is obtained within the IF-bandwidth of $B = 5$ MHz.

The I/N ratio within the IF-bandwidth B can be obtained by subtracting Eq. 6 from Eq. 4:

$$I/N = \frac{I_B}{N_B} \quad [dB] \quad \text{Eq. 7}$$

With :

The interference power I_B corresponding to the RNSS signal power S_B within the reference bandwidth B :

$$I_B = S_B = \int_{f_{Sat}-\frac{B}{2}}^{f_{Sat}+\frac{B}{2}} PSD(f) df \quad \text{Eq. 8}$$

The Power Flux Density, PFD at the antenna can be calculated from a given value for the carrier power C of the simulated interference signal as follows:

$$PFD = C + a_{Cab} + a_{Comb} - a_{WG} + S_{1M}/C - A_{eff} \quad [dB (W / (MHz \cdot m^2))] \quad \text{Eq. 9}$$

With:

S_{1M}/C : Quotient of the interference power $S_{1M}=I_{1M}$ according to Eq. 8 within a reference bandwidth of $B = 1$ MHz and the carrier power of the interference signal, in dB

Where:

$$S_{1M}/C = \frac{\int_{f_{Sat}-\frac{1}{2}MHz}^{f_{Sat}+\frac{1}{2}MHz} PSD(f) df}{C} \quad \text{Eq. 10}$$

A_{eff} : Effective antenna aperture in dBm^2 , calculated from the maximum antenna gain.

With:

$$A_{eff} = G \cdot \frac{I}{4p} \quad [m^2] \quad \text{Eq. 11}$$

For this application, the maximum gain of the pencil beam of 38.6 dBi, at the centre frequency of the Radar of 1259 MHz is used. This gives $A_{eff} = 15.15$ dBm^2 .

Tab. 7: Some characteristic parameters for the various satellite navigation signals

Signal Type	$1/f_c$ Spreading factor	S_{1M}/C Normalised 'power within signal bandwidth of 1 MHz'	S_B/C Normalised 'power within IF bandwidth $B = 5$ MHz'	S_B/S_{1M} Ratio of 'power within 5 MHz' and 'power within 1 MHz'
GLONASS C/A	-57.1 dB/Hz	-0.4 dB	-0.1 dB	0.3 dB
GPS C/A	-60.1 dB/Hz	-1.1 dB	-0.2 dB	0.9 dB
GPS P	-70.1 dB/Hz	-9.9 dB	-3.2 dB	6.7 dB
GALILEO E6	-73.1 dB/Hz	-12.7 dB	-5.8 dB	6.9 dB

The Equations Eq. 3 to Eq. 7 are in line with the methodology for the determination of interference to Radars from systems in other services described in ITU-R M.1461 [Ref. 5].

Since the I/N ratio is dependent on the reference bandwidth B, it is useful to convert the I/N ratio determined for one reference bandwidth B1 to the I/N ratio for a different bandwidth B2. It can be shown by using Eq. 6, 7 and 8 that this is done as follows:

Eq. 12

$$\frac{I_{B2}}{N_{B2}} \Big/ \frac{I_{B1}}{N_{B1}} = \frac{\int_{f_{Sat}-\frac{B2}{2}}^{f_{Sat}+\frac{B2}{2}} PSD(f) df}{\int_{f_{Sat}-\frac{B1}{2}}^{f_{Sat}+\frac{B1}{2}} PSD(f) df} \cdot \frac{B_1}{B_2} \quad [dB]$$

Using Eq. 10 and 12, one obtains the ratio between the I/N values for a reference bandwidth of 1 MHz and for 5 MHz for the various signal types the following values:

Tab. 8: Some characteristic parameters for the various satellite navigation signals

Signal Type	S_B/S_{1M}	5 MHz/ 1 MHz	$(I_{5M}/N_{5M})/(I_{1M}/N_{1M})$
	Ratio of 'power within 5 MHz' And 'power within 1 MHz'	Bandwidth ratio	Ratio of I/N values
GLONASS C/A	0.3 dB	7 dB	-6.7 dB
GPS C/A	0.9 dB	7 dB	-6.1 dB
GPS P	6.7 dB	7 dB	-0.3 dB
GALILEO E6	6.9 dB	7 dB	-0.1 dB

APPENDIX C – ABBREVIATIONS

ATC:	Air Traffic Control
BPSK:	Binary Phase Shift Keying
C/A:	Coarse/Acquisition Code of GPS or GLONASS
C:	Carrier Power
CFAR:	Constant False Alarm Rate
COHO	Coherent Oscillator
COSEC ² :	antenna beam with a Cosecans squared shape
E6:	One among other signal types of the European satellite navigation system GALILEO
f_c :	Code clock frequency of a satellite navigation signal
HPBW:	Half Power Beam Width
I/N:	ratio of Interference power and Noise power within the IF bandwidth
IF:	Intermediate Frequency
ITU:	International Telecommunication Union
k:	number of an individual channel of the GLONASS system
LNA:	Low Noise Amplifier
MDS:	Minimum Discernible Signal
MTD:	Moving Target Detection
P:	Precise Code of GPS or GLONASS
P_D :	Probability of Detection
P_{FA} :	Probability of False Alarm
PFD:	Power Flux Density
PN:	Pseudo Noise
PSD:	Power Spectral Density

RF:	Radio Frequency
Rpm:	Rotations Per Minute
S _{1M} :	Power within 1 MHz bandwidth
SASS-C:	Surveillance Analysis Support System for ATC Centre
SREM:	Surveillance Radar Equipment Medium range
STALO	Stabile Local Oscillator
STC:	Sensitivity Time Control

APPENDIX D – SELECTED MEASUREMENT RESULTS

GLONASS-L2 C/A

C (Signal Gen) dBm	C $a_{Cab}+a_{Comb}$ dB	C (LNA) dBm	C a_{WG} dB	C (Ant) dBm	S _B /C dB	S _B dBm	S _{1M} /C dB	S _{1M} (Ant) dBm	S _{1M} (Ant) dBm	A _{eff} dBm ²	PFD dBW (m ² MHz)	N _B dBm	S _B /N _B I/N dB	P _D undist. 55 min %	P _D dist. 55 min %	(dist. -undist.) 55 min % points	(dist. -undist.) 55 min absolute %
	-22		-5.7		-0.1		-0.4		30	15.2		-98					
-104		-126		-120.3		-120.4		-120.8	-150.8		-166		-22.4	89.41	90.44	1.03	0.00
-98		-120		-114.3		-114.4		-114.8	-144.8		-150		-16.4	89.97	91.52	1.55	0.58
-92		-114		-108.3		-108.4		-108.8	-138.8		-154		-10.4	90.86	91.21	0.35	-0.75
-86		-108		-102.3		-102.4		-102.8	-132.8		-148		-4.4	89.97	81.23	-8.74	-10.86
-80		-102		-96.3		-96.4		-96.8	-126.8		-142		1.6	89.85	78.05	-11.8	-14.28
-74		-96		-90.3		-90.4		-90.8	-120.8		-136		7.6	89.19	67.22	-21.97	-25.79
-68		-90		-84.3		-84.4		-84.8	-114.8		-130		13.6				

GPS-L2 C/A:

C (Signal Gen) dBm	C $a_{Cab}+a_{Comb}$ dB	C (LNA) dBm	C a_{WG} dB	C (Ant) dBm	S _B /C dB	S _B dBm	S _{1M} /C dB	S _{1M} (Ant) dBm	S _{1M} (Ant) dBm	A _{eff} dBm ²	PFD dBW (m ² MHz)	N _B dBm	S _B /N _B I/N dB	P _D undist. 55 min %	P _D dist. 55 min %	(dist. -undist.) 55 min % points	(dist. -undist.) 55 min absolute %
	-22		-5.7		-0.6		-1.1		30	15.2		-98					
-104		-126		-120.3		-120.9		-122	-152		-167.2		-22.9	92.03	93.9	1.87	0.00
-98		-120		-114.3		-114.9		-116	-146		-161.2		-16.9	89.8	90.29	0.49	-1.54
-92		-114		-108.3		-108.9		-110	-130		-155.2		-10.9	91.98	91.38	-0.6	-2.69
-86		-108		-102.3		-102.9		-104	-134		-149.2		-4.9	91.15	89.72	-1.43	-3.62
-80		-102		-96.3		-96.9		-98	-128		-143.2		1.1	92.27	84.83	-7.44	-10.09
-74		-96		-90.3		-90.9		-92	-122		-137.2		7.1	90.09	72.34	-17.75	-21.78
-68		-90		-84.3		-84.9		-86	-116		-131.2		13.1				

GPS-L2 P:

C (Signal Gen) dBm	C $a_{Cab}+a_{Comb}$ dB	C (LNA) dBm	C a_{WG} dB	C (Ant) dBm	S _B /C dB	S _B dBm	S _{1M} /C dB	S _{1M} (Ant) dBm	S _{1M} (Ant) dBm	A _{eff} dBm ²	PFD dBW (m ² MHz)	N _B dBm	S _B /N _B I/N dB	P _D undist. 55 min %	P _D dist. 55 min %	(dist. -undist.) 55 min % points	(dist. -undist.) 55 min absolute %
	-22		-5.7		-3.2		-9.9		30	15.2		-98					
-104		-126		-120.3		-123.5		-130.2	-160.2		-175.4		-25.5				
-98		-120		-114.3		-117.5		-124.2	-154.2		-169.4		-19.5	91.55	91.89	0.34	0.00
-92		-114		-108.3		-111.5		-118.2	-148.2		-163.4		-13.5	89.91	90.78	0.87	0.59
-86		-108		-102.3		-105.5		-112.2	-142.2		-157.4		-7.5	92.49	92.49	0.00	-0.37
-80		-102		-96.3		-99.5		-106.2	-136.2		-151.4		-1.5	90.11	89.93	-0.18	-0.58
-74		-96		-90.3		-93.5		-100.2	-130.2		-145.4		4.5	92.77	89.88	-2.89	-3.48
-68		-90		-84.3		-87.5		-94.2	-124.2		-139.4		10.5	91.68	81.33	-10.35	-11.66

GALILEO E6:

C (Signal Gen) dBm	C $a_{Cab}+a_{Comb}$ dB	C (LNA) dBm	C a_{WG} dB	C (Ant) dBm	S _B /C dB	S _B dBm	S _{1M} /C dB	S _{1M} (Ant) dBm	S _{1M} (Ant) dBm	A _{eff} dBm ²	PFD dBW (m ² MHz)	N _B dBm	S _B /N _B I/N dB	P _D undist. 55 min %	P _D dist. 55 min %	(dist. -undist.) 55 min % points	(dist. -undist.) 55 min absolute %
	-22		-5.7		-5.8		-12.7		30	15.2		-98					
-104		-126		-120.3		-126.1		-133	-163		-178.2		-28.1				
-98		-120		-114.3		-120.1		-127	-157		-172.2		-22.1	92.06	92.26	0.2	0.00
-92		-114		-108.3		-114.1		-121	-151		-166.2		-16.1	91.09	91.7	0.61	0.45
-86		-108		-102.3		-108.1		-115	-145		-160.2		-10.1	92.37	92.92	0.55	0.38
-80		-102		-96.3		-102.1		-109	-139		-154.2		-4.1	91.41	92.22	0.81	0.67
-74		-96		-90.3		-96.1		-103	-133		-148.2		1.9	93.3	90.09	-3.21	-3.65
-68		-90		-84.3		-90.1		-97	-127		-142.2		7.9	91.31	85.68	-5.63	-6.38

For explanation of abbreviations refer to Appendix B